# Efficient Algorithms for Mobile Sink Aided Data Collection From Dedicated and Virtual Aggregation Nodes in Energy Harvesting Wireless Sensor Networks

Lei Tao, Xin Ming Zhang, *Senior Member, IEEE*, and Weifa Liang, *Senior Member, IEEE*

***Abstract*—We study the mobile data collection problem in an energy harvesting wireless sensor network (EH-WSN), where sensor nodes are densely deployed in a monitoring area and a mobile sink (MS) travels around the area to collect sensory data from the sensors. In order to optimize the network performance while achieving perpetual network operation, we propose efficient algorithms to dynamically schedule the MS for collecting data from sensors with different data generation rates. Specifically, in this paper, we propose an optimization framework that consists of three stages. We first deal with the reliable, stable, and energy neutral energy assignment for sensors. We then find a closed trajectory for the MS for sensory data collection that covers as many as aggregation nodes, and devise a decentralized algorithm to determine the data generation rate of each sensor and the data flow rate of each link to optimize the network performance. We also develop a fast heuristic algorithm for the problem. We finally evaluate the performance of the proposed algorithms through numerical experiments. The simulation results demonstrate that the proposed algorithms are efficient.**

***Index Terms*—Distributed algorithms, energy harvesting wireless sensor networks, network utility, mobile data collection, path planning.**

## I. Introduction

SINK mobility [1] has been proven to be an effective technique that facilitates balancing energy consumption among sensor nodes and prolongs the lifetime of battery-operated wireless sensor networks (WSNs). In a mobile data collection framework, some sensor nodes are identified as aggregation nodes to gather sensory data for the other sensors. A mobile sink (MS) moves to the vicinity of the aggregation nodes to collect data from them. The aggregation nodes then distribute data traffic that intended route to a static sink across the network, to achieve energy balance among sensor nodes and balanced traffic distribution [2]. On the other hand, energy harvesting (EH) [3] is another efficient technology that enables sensor nodes to harvest ambient energy (solar, wind, etc) from their surrounding environments, which has been paid more attention recently due to its features of environmental friendliness, free replacements for batteries, and potential to achieve perpetual network operation.

The adoptions of EH technique and sink mobility pose challenges for mobile data collection. The mobile data collection problem usually involves two issues, including the data collection path planning for the MS, and the data routing optimization for sensors, which are together coupled with the energy harvesting profile of each sensor. For example, the trajectory of an MS impacts how sensors can efficiently route their sensory data to the MS. Also, data generation rates and the data routing path primarily determine the energy consumption of an individual sensor node, which should be constrained by the battery level and energy harvesting rate of the sensor, in order to prolong network lifetime. Handling the dynamics of harvested energy and energy usages of sensors need efficient optimization algorithms, and tackling the mobile data collection problem with various constraints requires novel optimization frameworks.

Several studies [4]–[8], [12] have investigated the benefits of sink mobility to data collection in an energy renewable network. The authors in [4]–[7] assumed that the trajectory of data collection of an MS is predetermined. However, a fixed data collection path is not applicable to the time-varying energy profiles of sensor nodes. To handle this problem, Guo *et al.* [8] and Wang *et al.* [12] proposed algorithms that first dynamically choose aggregation nodes according to the predicted energy harvesting rate of each sensor, and then plan a data collection trajectory for the MS that traverses on these aggregation nodes. However, the benefit of sink mobility has not been fully explored. In this paper, we consider that if the MS is within the transmission range of a sensor node with data to upload, the MS could directly collect the data from the sensor node. We use an example in Fig. 1 to explain the

Manuscript received December 28, 2018; revised April 25, 2019; accepted July 6, 2019. Date of publication July 9, 2019; date of current version November 20, 2019. This work was supported in part by the National Key Research and Development Program of China under Grant 2017YFC0804402, in part by the National Natural Science Foundation of China under Grant 61672485 and Grant 61379130, in part by the Open Research Fund of National Mobile Communications Research Laboratory, Southeast University under Grant 2019D13, and in part by the Anhui Initiative in Quantum Information Technologies under Grant AHY150300. The associate editor coordinating the review of this paper and approving it for publication was V. Y. F. Tan.
*(Corresponding author: Xin Ming Zhang.)*

L. Tao and X. M. Zhang are with the School of Computer Science and Technology, University of Science and Technology of China, Hefei 230027, China, and also with the National Mobile Communications Research Laboratory, Southeast University, Nanjing 210096, China (e-mail: taolei@mail.ustc.edu.cn; xinming@ustc.edu.cn).

W. Liang is with the Research School of Computer Science, Australian National University, Canberra, ACT 2601, Australia (e-mail: wliang@cs.anu.edu.au).

Digital Object Identifier 10.1109/TGCN.2019.2927619

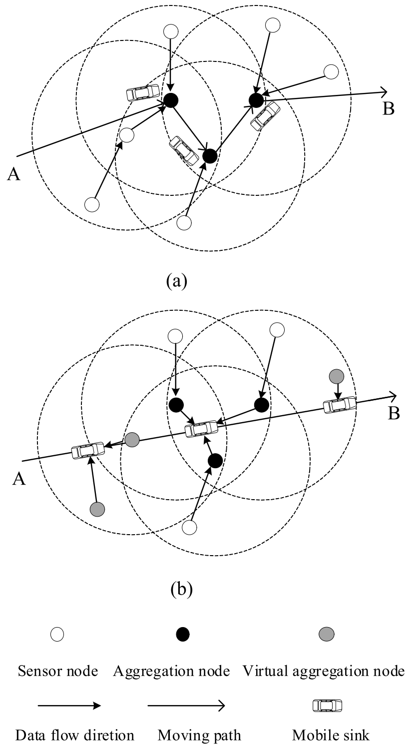


Fig. 1. (a) Traditional and (b) proposed mobile data collection strategies.

data collection mechanism. We consider a segment of the data collection trajectory from point A to point B. A dashed circle indicates the communication range of a node. In Fig. 1(a), the MS traverses each aggregation node to collect data from the shown sensors. However, with the proposed transmission strategy in Fig. 1(b), the MS just needs to go through the overlapped coverage area of the communication ranges of the aggregation nodes. As a result, the movement distance from A to B is reduced compared to Fig. 1(a). Moreover, we let virtual aggregation nodes transmit data directly to the passing-by MS instead of via aggregation nodes, where virtual aggregation nodes are defined as the sensors near the trajectory of the MS and do not relay data for other sensors. With the help of virtual aggregation nodes, the load of relayed data for the dedicated aggregation nodes decreases, in other words, these aggregation nodes can transmit more data with constrained energy, which help to yield a better network performance.

In this paper, we investigate the mobile data collection problem with the aim of maximizing network utility in an MS aided energy harvesting sensor network, subject to various coupled constraints such as the traveling length constraint on the MS and constraints on link and battery capacity on sensors. The main contributions of this paper are summarized as follows.

We mathematically formulate a mobile data collection problem. We first propose a harvested energy arrangement policy that dynamically assigns the energy budget to sensors according to time-varying energy harvesting rates, which can avoid energy deficit and energy overflow occurring. We then develop an algorithm that effectively identifies aggregation nodes and finds a closed data collection trajectory that covers the elected aggregation nodes, subject to the trajectory length. Also, we devise a fully distributed algorithm to maximize the network utility with the given energy budget and constraints on links, where we allow virtual aggregation nodes near the data collection trajectory to upload their data directly to the MS when it passed by. Finally, we conduct numerical evaluation on the performance of the proposed algorithms. Experimental results demonstrate that the proposed algorithms are efficient.

The rest of this paper is organized as follows. The related work is surveyed in Section II. Section III defines the scope of our problem and outlines our solutions. Section IV proposes the algorithms of energy budget assignment, mobile data collection trajectory planning, and sensors data rate and link flow rate optimization. Section V provides the simulation results. The paper concludes in Section VI.

## II. Related Work

There have been serval studies on network performance optimization of data collection in energy harvesting sensor networks [13]–[19]. For example, Zhang *et al.* [13] proposed a distributed data gathering approach to maximize the network utility in terms of total amount of data collected by the MS, while maintaining network fairness. Here, fairness means the data generation rate of each sensor node should not vary significantly. Chen *et al.* [14] addressed the joint optimization problem of energy allocation and routing to maximize the total system utility, without prior knowledge of the replenishment profile of each sensor. A low-complexity online solution is also proposed that achieves asymptotic optimality. Focusing on the purposes of network utility maximization and perpetual network operation, Liu *et al.* [15] developed a dual decomposition and subgradient based algorithm, called QuickFix, to compute the optimal data sampling rate and route, and a SnapIt algorithm to adjust the sampling rate. Lin *et al.* [16] developed routing algorithms to optimally maximize the throughput and available energy in the presence of energy constraints with no statistical information on packet arrivals. Taking into account the dynamic feature of network topology, Zhang *et al.* [17] designed a data gathering optimization algorithm called DoSR for dynamic sensing and routing. An improved algorithm to manage the energy allocation in dynamic environments and a topology control scheme was also proposed to reduce computational complexity. Aoudia *et al.* [18] formulated the packet generation rates (PGR) maximization a convex problem and adopted a fast version of the ADMM to distributively compute optimal and fair packet rates in energy harvesting sensor networks. Yang and McCann [19] studied the optimal lexicographic max-min (LM) rate allocation problem in solar-powered wireless sensor networks, to achieve both LM optimality and sustainable operation.

Also, several recent studies [4]–[8], [12], [20] considered both the rechargeable characteristic of sensors and sink mobility to further improve the network performance. In [4], [5], the throughput maximization problem was investigated in energy harvesting sensor networks, where an MS traverses along a fixed path to collect data from sensors within one-hop distance. Deng *et al.* [6] proposed a distributed algorithm to jointly optimize the data sampling rates and battery levels to maximize the network utility with spatiotemporally-coupled constraints in rechargeable sensor networks. Zhang *et al.* [7] extended their work in [13] to an MS aided scenario and proposed near optimal distributed data gathering schemes in EH-WSNs. Until now, the aforementioned work assumes that the trajectory of the MS is pre-determined. To further adapt the dynamics of energy harvesting sensor networks, Zhao *et al.* [20] investigated an optimization framework to jointly achieve mobile energy replenishment and data gathering in rechargeable sensor networks. Period-wise data collection and recharging path is calculated on-demand based on the battery state of sensors. And the authors devised a distributed algorithm to achieve flow-level network utility maximization. Guo *et al.* [8] extended the work in [20] by considering heterogeneous energy consumption of sensors and time-varying charging duration, and proposed distributed cross-layer strategy, which adaptively adjusts the optimal rate, routing paths, instant energy provisioning status, and charging durations to maximize the network utility. Wang *et al.* [12] investigated the mobile data gathering problem in EH-WSNs by a two-step approach where data collection trajectory for the MS and source plus flow rates for the sensors are optimized in each step, respectively. The influence of shadows on the solar profiles is emphasized in this work.

In the area of unmanned aerial vehicle (UAV) communication and trajectory design, Zhan *et al.* [21] studied energy-efficient mobile data collection in an UAV aided WSN. Zeng and Zhang [22] proposed a point-to-point UAV-to-single-base-station communication and UAV trajectory planning algorithm. In [21], [22], a novel approximation method based on Taylor expansion was adopted that relaxs a non-convex problem into a convex optimization problem. Ho *et al.* [23] focused on the energy efficiency problem, and proposed a Low Energy Adaptive Clustering Hierarchy (LEACH)-based protocol. A Particle Swarm Optimization (PSO) method was proposed to find the optimal topology in order to reduce the energy consumption, bit error rate (BER), and UAV travel time.

Unlike the aforementioned studies, in this paper we study a dynamic mobile data collection problem that plans a trajectory for the MS and optimizes data generation rates for sensors, where dedicated and virtual aggregation nodes are used to transmit data to the MS to fully utilize the opportunities of data uploading.

## III. Preliminaries

### A. System Model

We consider an EH-WSN with node set $\mathcal{N}' = \mathcal{N} \cup \{s\}$, where $\mathcal{N}$ is a set of $n$ homogeneous stationary sensor nodes that are deployed over a monitoring area and $s$ represents an MS node. We use the term node to refer either a sensor node or an MS node. Each sensor is equipped with renewable energy supply (e.g., solar energy), stores and generates sensory data to upload. The sensory data rate of a sensor node is called its data generation rate. The sink node is a vehicle, e.g., a mobile car or an unmanned aerial vehicle, that moves periodically through the monitoring area to collect data from sensors.

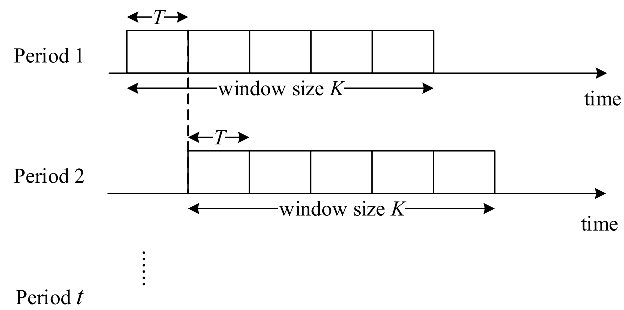


Fig. 2. The dynamic mobile data collection optimization process.

Time is divided into equal time periods/durations of length $T$. Without loss of generality, we assume that an MS completes a closed mobile data collection trajectory once per time period. In each period, we aim to optimize the network performance over the next $K$ periods, as depicted in Fig. 2. And each time the time period index is increased by one, with one more period harvested energy prediction information, we will rerun the optimization algorithms based on the energy usage at previous time period. Therefore, the mobile data collection optimization problem is a dynamic problem.

### B. Mobile Data Collection

In each data collection trajectory, each sensor node first forwards its data to an aggregation node (or several aggregation nodes) through one-hop or multi-hop transmission, and the MS stops at some positions called *collection centers* for a certain amount of time to gather data from its neighboring aggregation node(s). We use $\mathcal{C}(t)$ and $\mathcal{A}(t)$ to indicate the set of collection sites and of aggregation nodes, respectively, and use $\sigma_u$ to represent the stop time of the MS at collection center $u \in \mathcal{C}(t)$.

The aggregation nodes and data collection trajectory design should satisfy that the MS traverses the areas within the communication range of each chosen aggregation node in order to collect data from it. We let

$$\chi_u(t) := \{i \in \mathcal{A}(t) \mid d(p_i, p_u) \leq R\}, \tag{1}$$

where $p_u$ and $p_i$ denote the coordinate of a collection center $u$ and an aggregation node $i$, respectively. $d(\cdot,\cdot)$ denotes the distance between two coordinates. Then the following should be satisfied

$$\chi_u(t) \neq \emptyset, \ \forall u \in \mathcal{C}(t). \tag{2}$$

Constraint (2) means that for each collection center $u$ on the trajectory, $u$ should be within the transmission range of a certain aggregation node, so that the MS is able to collect data from the aggregation nodes.

Also, the length of the data collection trajectory reflects the total amount of time and energy consumption of the MS to complete a data collection trajectory, we bound the total length of all data collection trajectories over all time periods by $l_b$.

The sum trajectory lengths constraint can be expressed as:

$$\sum_{t\in\mathcal{K}} l(t) \le l_b, \tag{3}$$

where *l*(*t*) denotes the length of the mobile data collection trajectory in time period *t*.

Once a data collection trajectory is determined at a certain period *t*, the sensors near the trajectory can choose to transmit data directly to the MS when the MS passes by without influencing its traveling speed. We call these wayside sensors virtual aggregation nodes and denote the set of virtual aggregation nodes by $\mathcal{W}(t)$.

### C. Energy Model

For the energy supply model, we assume an energy predictor [18] that can provide predictions of harvested energy over each time period and use $h_i(t)$ to represent the average energy harvesting rate of sensor node *i* at time period *t*. And for the energy cost model, we assume that transmitting, receiving and sensing data dominate the energy consumption of each sensor. We use $e^{tx}$, $e^{rx}$ and $e^{s}$ to indicate the energy costs for transmitting, receiving and sensing one bit of data, respectively. In period *k*, assume the data generation rate of sensor *i* is $r_i(t)$, and the data flow rate at a link *l* is $f_l(t)$. The energy cost of sensor *i* at time period *t* can be expressed as:

$$c_i(t) = \sum_{l\in\mathcal{O}_i(t)} e^{tx} f_l(t) + \sum_{m\in\mathcal{I}_i(t)} e^{rx} f_m(t) + e^{s} r_i(t), \forall i \in \mathcal{N}, \tag{4}$$

where $\mathcal{O}_i(t)$ and $\mathcal{I}_i(t)$ represent outgoing links and incoming links of sensor *i* at time period *t*, respectively. Note that $\mathcal{O}_i(t)$ and $\mathcal{I}_i(t)$ are optimization variables.

We adopt the harvest-store-use (HSU) model [3]. The recurrence expression of the battery level at sensor node *i* at time period *t* can be expressed as

$$b_i(t) = [b_i(t-1) - (a_i(t) - h_i(t))T]^+, \ \forall t \in \mathcal{K}, \tag{5}$$

where $a_i(t)$ represents the energy budget of sensor node *i* at time period *t*. *B* is the maximum capacity of the battery of a sensor node. $[x]^+ := \min(B, \max(0, x))$.

### D. Link Model

We consider a time division multiple access (TDMA) system for data transmission. Assume that a node cannot transmit to or receive from multiple nodes simultaneously, and cannot perform both transmission and reception simultaneously [33], we have the following constraint:

$$\sum_{l\in\mathcal{O}_i(t)} \frac{f_l(t)}{\pi_l} + \sum_{m\in\mathcal{I}_i(t)} \frac{f_m(t)}{\pi_m} \le 1, \ \forall i \in \mathcal{N}, \tag{6}$$

where $\pi_l$ is the bandwidth capacity of link *l*. We classify the links $\mathcal{L}$ into three categories. A link exists between any two sensor nodes if they are within transmission range of each other, between each aggregation node and the MS, and between each virtual aggregation node and the MS if the distance of the node to the mobile data collection trajectory is no larger than *R*. We call the first category a S2S link, which means a link from a sensor to anther sensor, and call the second and third categories as V2MS link and as A2MS link, respectively, which mean links from a virtual aggregation node and an aggregation node to the MS.

The information flow conservation condition is described as follows:

$$\sum_{l\in\mathcal{O}_i(t)} f_l(t) - \sum_{m\in\mathcal{I}_i(t)} f_m(t) - r_i(t) = 0, \ \forall i \in \mathcal{N}. \tag{7}$$

Constraint (7) ensures that the incoming data flows plus the source flow equals the outgoing data flows to the aggregation node(s).

### E. Problem Formulation

The mobile data collection problem can be described as planning data collection trajectories for the MS that includes selecting aggregation nodes, and optimizing data generation rates of sensors and data flow rates for links over time intervals with energy neutral constraint, link capacity constraints, battery constraints and trajectory length constraint. We formulate the mobile data collection problem as follows.

$$\mathbf{P}: \max_{\boldsymbol{r},\boldsymbol{f},\boldsymbol{A},\boldsymbol{C},\boldsymbol{\sigma}} \sum_{t\in\mathcal{K}} \sum_{i\in\mathcal{N}} \log(r_i(t)), \tag{8}$$

$$\text{subject to} \quad \text{Constraints (2), (3), (6), (7)}$$

$$\frac{l(t)}{v} + \sum_{u\in\mathcal{C}(t)} \sigma_u \le T, \ \forall t, \tag{9}$$

$$b_i(t) \ge 0, \ \forall i, t, \tag{10}$$

$$b_i(K) \ge b_i^n, \ \forall i, \tag{11}$$

where $\boldsymbol{r} := \{r_i(t) \mid i \in \mathcal{N}, t \in \mathcal{K}\}$, $\boldsymbol{f} := \{f_l(t) \mid l \in \mathcal{L}', t \in \mathcal{K}\}$, $\boldsymbol{A} := \{\mathcal{A}(t) \mid t \in \mathcal{K}\}$, $\boldsymbol{C} := \{\mathcal{C}(t) \mid t \in \mathcal{K}\}$ and $\boldsymbol{\sigma} := \{\sigma_u(t) \mid u \in \mathcal{C}(t), t \in \mathcal{K}\}$ are the optimization variables. Note the unit of data generation rate $\boldsymbol{r}$ and the data flow rate $\boldsymbol{f}$ are both kbps. The *utility function* of the network is defined as the sum of logarithmic function $\log(\cdot)$ of sensors' sensory data generation rates over time, which achieves proportional fairness [31] among sensor nodes. Constraint (9) ensures that the duration of a mobile data collection trajectory does not exceed the monitoring period *T*. Constraints (10) and (11) guarantee that a sensor never exhausts its energy and its battery level should be greater than a given threshold $b_i^n$ in the end of the periods.

## IV. Optimization Algorithms for the Mobile Data Collection Problem

Tackling problem P is very difficult due to the following reasons. First, the trajectory planning problem is a decisional version of the NP-hard Traveling Salesman Problem (TSP), in which data collection trajectory needs to be found that traverses all collection centers with bounded length. Second, it is computation-inefficient to enumerate all the possible combination of aggregation nodes from all sensors in the network at each time period.

We devise an optimization framework for the problem, as depicted in Fig. 3. The proposed framework consists of three

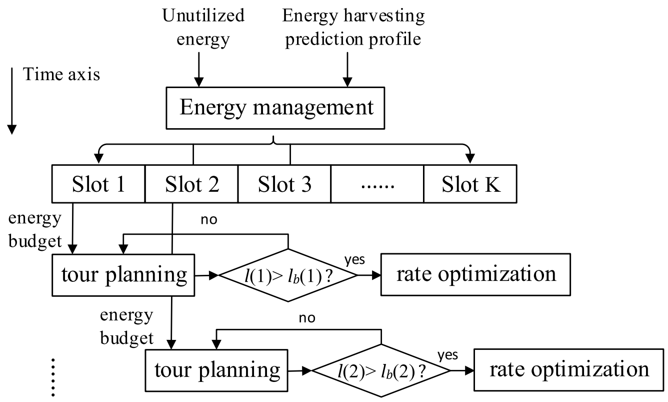


Fig. 3. An overview of the optimization framework.

stages. In the top layer, we perform an efficient energy management strategy to decide a feasible energy budget for each sensor over time periods with harvested energy under the battery capacity constraint. In the lower layers, we first adopt a progressive algorithm to plan a data collection trajectory for the MS under the trajectory length constraint and traveling time constraint. We gradually increase the number of collection centers and plan a closed trajectory that covers these collection centers, while the length of the trajectory is no larger than $l_b(t)$. Here, $l_b(t)$ is the trajectory length bound in time period *t*. How to obtain $l_b(t)$ will be discussed in the following. We meanwhile determine the stop time at each collection site for the MS. When we obtain the dedicated and virtual aggregation node set based on the planned trajectory, we finally propose a distributed algorithm that optimizes data generation rates and link flow rates with the provided energy budget to maximize the network utility.

The motivation behind the proposed optimization framework in Fig. 3 is explained as follows. The overall optimization problem includes determining data flow rates related to links, data generation rates of sensors, and data collection trajectory of the MS with energy, link capacity and trajectory length constraints. As the problem is a complicated joint optimization problem, we decouple it into several optimization sub-problems. The decoupling method should satisfy the following principles. First, the trajectory of the MS must be planned before data flow rates and data generation rates optimization because only after the trajectory of the MS is decided, we can determine which nodes are selected as aggregation nodes, and then can flow rates and data generation rates optimization be conducted. We perform harvested energy budget allocation at the beginning of the framework for the purpose of mitigating the impact of spatiotemporal-varying energy harvesting profile and achieve balanced performance over time. The network performance relies heavily on the energy harvesting profile and real-time battery state and could be unstable without proper energy management strategy. Therefore, we first decouple the energy constraints to perform efficient energy management for sensors, after that, we plan the data collection trajectory for the MS, which could potentially yield better network performance, and finally we conduct flow rates and data generation rates optimization.

### *A. Harvested Energy Management*

We consider the management of harvested energy for each sensor node. We assume that the monitoring time window consists of *K* time periods. We consider an energy management scheme that is reliable, efficient, energy neutral and stable. Specifically, reliability means that each node never runs out of battery under the energy allocation scheme. Efficient energy management aims to minimize the energy waste, which is the amount of energy that fails to store into a battery due to its limited capacity. Maintaining energy neutrality means that, at the end of the time periods, the battery level should be greater than the defined battery neutrality level $b_i^n$. Stability represents that the variance of allocated energy in each period is minimized, the consideration behind which is that we try to achieve steady network performance over time from the perspective of energy allocation, when the harvested energy could vary significantly over time, e.g., the solar harvesting rate is high near noon, however, low at morning and at dusk. The energy assignment problem for each sensor *i* is formulated as follows:

$$\begin{aligned} \mathbf{P1}: \min_{\boldsymbol{a}_i} \quad & (a_i(t) - \overline{a_i}(t))^2, && (12)\\ \text{subject to} \quad & a_i(t) - b_i(t-1) - h_i(t) \le 0, && (13)\\ & b_i(t-1) + h_i(t) - a_i(t) - B \le 0, && (14)\\ & b_i(K) - b_i^n = 0, && \\ & \forall t \in \mathcal{K}, && (15) \end{aligned}$$

where $\overline{a_i}(t) = \frac{1}{K}\sum_{t=1}^{K} a_i(t)$. Note that in constraint (14), we determine that the battery level should not exceed *B*, which abandons the waste of harvested energy.

Let $b_i(0)$ to represent the initial battery level of sensor node *i*, we have

*Lemma 1:* The battery level of sensor node *i* can be expressed by $b_i(t) = b_i(0) + \sum_{k=1}^{t}(h_i(k) - a_i(k))$ for any time period *t* under constraint (5), (13) and (14).

*Proof:* We first take off the operator $[\cdot]^+$ by proving $b_i(t) = b_i(t-1) - a_i(t) + h_i(t)$ for $\forall t$. For $t = 1$, $b_i(1) = \min(B, \max(0, b_i(0) - a_i(1) + h_i(1))) \overset{(a)}{=} \min(B, b_i(0) - a_i(1) + h_i(1)) \overset{(b)}{=} b_i(0) - a_i(1) + h_i(1)$, where (*a*) holds by equation (13) and (*b*) holds by equation (14). Then we can derive $b_i(t) = b_i(t-1) - a_i(t) + h_i(t) = b_i(t-2) - [a_i(t) + a_i(t-1)] + [h_i(t) + h_i(t-1)] = \cdots = \cdots b_i(0) + \sum_{k=1}^{t}(h_i(k) - a_i(k))$. ■

By Lemma 1 and Eq. (15), we have $\sum_{t\in\mathcal{K}} a_i(t) = \sum_{t\in\mathcal{K}} h_i(t)$. Constitute the conclusion of Lemma 1 into Equations (13) and (14), we can formulate an equivalent problem to P1 as:

$$\mathbf{P2}: \min_{\boldsymbol{a}_i(t)} \sum_{t\in\mathcal{K}} a_i^2(t) - \frac{1}{K}(\sum_{t\in\mathcal{K}} h_i(t))^2, \quad (16)$$

$$\text{subject to} \sum_{k=1}^{t} h_i(t) + b_i(0) - B \le \sum_{k=1}^{t} a_i(t) \le \sum_{k=1}^{t} h_i(t) + b_i(0), \forall t \in \mathcal{K}. \quad (17)$$

Since term $-\frac{1}{K}(\sum_{t\in\mathcal{K}} h_i(t))^2$ in Eq. (16) is a constant, we are in fact solving a quadratic program (QP) in terms of $\boldsymbol{a}_i$ with linear inequality constraint, and there are polynomial-time interior-point algorithm [25] for it. According to the experimental results, when $K$ is set to 12, the proposed algorithm converges averagely within around 5 iterations. Thus, the computational overhead is acceptable for a sensor node.

### B. Mobile Data Collection Trajectory Planning

With the energy budget assigned to each sensor over time, the next question is to identify a data collection trajectory for the MS at each time period. We need to determine aggregation nodes, data collection trajectory and collection centers simultaneously. In order to maximize the data collected at each time period, the number of qualified aggregation nodes should be as many as possible. Intuitively, a sensor with more allocated energy should be assigned a higher weight $w_i$ in the selection of aggregation nodes, e.g.,

$$w_i(t) = a_i(t). \tag{18}$$

Since aggregation nodes generally consume more energy than non-aggregation nodes, the preference for electing sensors with less allocated energy as aggregation nodes exacerbates the unbalance and underutilization of allocated energy and decreases the network utility. Similar but different from [20] where the remaining energy of a sensor is regarded as the weight, we use the allocated energy as weight and achieve network-wide energy balance at a higher level by maintaining energy neutral for each sensor.

Nevertheless, the increase on the number of aggregation nodes result in the increase in length of the data collection trajectory. We set the trajectory length of the MS at time period $t$ no greater than $l_b(t)$. $l_b(t)$ should satisfy that the sum of $l_b(t)$ over all time periods cannot exceed the total trajectory length constraint $l_b$. Since we need to handle joint the MS trajectory optimization and the network resources optimization, the following method is adopted to tailor the sum trajectory length constraint into each time period. Given the sum trajectory length constraint $l_b$, the MS trajectory constraint in time period $t$ is represented by

$$l_b(t) = \frac{\sum_i a_i(t)}{\sum_i \sum_t a_i(t)} l_b. \tag{19}$$

The weighted-average in Eq. (19) implies that when the network is allocated with more energy budget at a certain period $t$, i.e., $\sum_i a_i(t)$ becomes large, then the sum of data generation rates of sensor nodes is large as well. Therefore, the MS is allowed to travel longer in order to collect more data from the sensor nodes.

We propose the following method to identify aggregation nodes. First, all the sensors are ranked in ascending order regarding $w_i(t)$ and only the first sensor is included into the aggregation node set $\mathcal{A}(t)$. Next, we solve the Traveling Salesman Problem with Neighborhoods (TSPN) [9] for sensors in $\mathcal{A}(t)$, the trajectory length $l(t)$ and the position of collection centers are then obtained. We gradually increase the size of the aggregation nodes set until $l(t)$ approaches $l_b(t)$. Moreover, we adopt *binary search* to accelerate the election process. A data collection trajectory with bounded length is finally obtained.

In order to solve the TSPN with a given aggregation node candidate set $\mathcal{A}$, a basic mechanism that heuristically tackle a TSPN is given as follows. First, we search for a set of collection centers to represent the set of aggregation nodes, with each collection center covering as many as aggregation nodes, so that the number of collection centers can be significantly reduced. Next, we apply an approximation algorithm for TSP to form a trajectory that connects all the collection centers. We further reduce the length of the trajectory without violating the constraint that the trajectory should intersect with the communication disks of virtual aggregation sensors. We adopt a combination algorithm [10] to calculate the collection centers, which was originally designed to reduce the length of a TSPN trajectory for data collection. With identified aggregation nodes, the algorithm identifies collection centers greedily that cover the maximum number of aggregation nodes, then these covered aggregation nodes are removed from the aggregation node set. The algorithm continues until the aggregation node set is empty.

We then further reduce the trajectory length by adjusting the position of collection centers, where we distinguish three cases as illustrated in Fig. 4. We use $p_{j-1}$, $p_j$ and $p_{j+1}$ to denote three sequential collection center points on the trajectory, where $p_j$ is the collection center to adjust. In cases 1 and 2, the segment $\overline{p_{j-1}p_{j+1}}$ does not intersect with the communication disk(s) of the sensor(s) that $p_j$ covers, and the difference between these two cases is that whether $p_j$ covers one or multiple sensors. In case 3, $\overline{p_{j-1}p_{j+1}}$ intersects with the aforementioned communication disk(s).

*Case 1:* as depicted in Fig. 4(a), we aim to minimize the sum of lengths $\overline{p_{i-1}p_i^*}$ and $\overline{p_i^*p_{i+1}}$, where $p_i^*$ is constrained within the area formed by circle A. We find out $p_i^*$ by the following lemma.

*Lemma 2:* We formulate an ellipse C with two focal points $p_{j-1}$ and $p_{j+1}$ that are externally tangent with circle A, then $p_i^*$ is a tangency point.

*Proof:* According to the definition of an ellipse, for each point $p$ on C we have $\overline{p_{j-1}p} + \overline{pp_{j+1}} = 2a$, where $2a$ is the length of long shaft. We gradually increase $a$ until C is right tangent with A and obtains the tangency point $p_i'$, then any other points $p_i''$ on A is outside the area formed by C, which means $p_i'$ corresponds to a ellipse with larger long shaft $a'$, e.g., $\overline{p_{j-1}p_i''} + \overline{p_i''p_{j+1}} > \overline{p_{j-1}p_i^*} + \overline{p_i^*p_{j+1}}$, thus $p_i'$ is the optimal point. ■

*Case 2:* as shown in Fig. 4(b), the situation becomes more complicated owing to the irregular public coverage area formed by serval communication disks. However, noticing the fact that $p_i^*$ is either a tangent point or one of the intersection points of the arcs that form the area, the following method is adopted to work out $p_i^*$. We label the public coverage area as A$'$. At first, each arc that makes up A$'$ is calculated. For each arc we have a circle it belongs to, for which we apply the algorithm for case 1 to find out the tangent point. The tangent point is regarded as qualified if it is on the corresponding

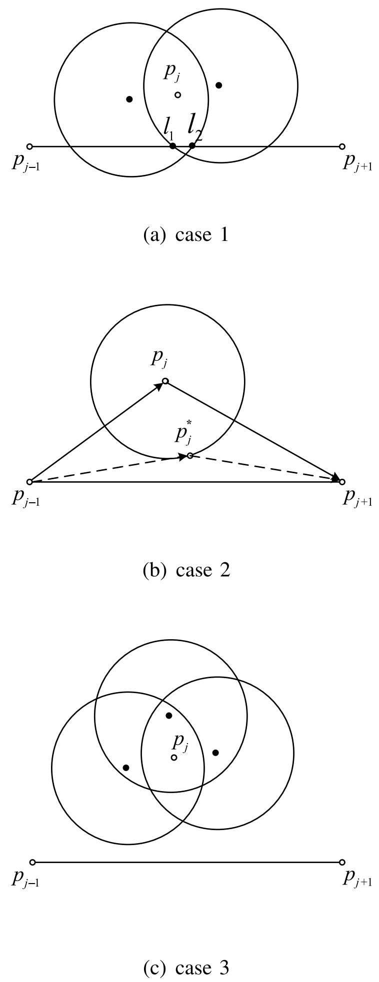


Fig. 4. Shorten the length of a path within the trajectory by adjusting the position of the collection center $p_j$ in different cases.

arc, and if it is, the length of the corresponding path is calculated and recorded. Finally, we find the minimum-length paths from the record, and obtain $p_j^*$, which is the associated tangent point. Otherwise, if no tangent point is qualified, then $p_j^*$ must be one of the intersection points. Then, the length of path in terms of each intersection point is compared, $p_j^*$ is the one with the minimum path length.

*Case 3:* a special case where the short shaft length of C is zero. Since all the feasible positions of $p_j^*$ lead to the same path length, we select one of the position randomly on the intersection segment $\overline{l_1 l_2}$ as $p_j^*$.

The aforementioned optimization is repeatedly adopted until the position of each collection center is adjusted. Since the length of the path that constitutes the trajectory is shortened in each step, the total length of the collection trajectory decreases in the end.

Similarly, we decide the stop time $\sigma_u(t)$ at each collection site *u* based on the energy assignment weight *w*(*t*). The remaining time for the MS to stop and collection data at a collection site is

$$t_r = T - \frac{l(t)}{v}, \ \forall t \in \mathcal{K}. \tag{20}$$

We let the stop time be

$$\sigma_u(t) = t_r \frac{\sum_{i \in \chi_u} w_i(t)}{\sum_{j \in \mathcal{A} \setminus \chi_u} w_j(t)}. \tag{21}$$

The insight behind is that when more aggregation nodes with rich energy are covered by the collection site *u*, more sensory data can be routed to *u*. Therefore, the MS should stop at *u* a bit longer in order to collect more data.

*Discussions:* We consider the influence of obstacles in the network and study its influence on the construction of the MS trajectory. The obstacles can impact the construction of a TSP trajectory and the adjustment of the trajectory. For the construction of a TSP trajectory, existing studies proposed different schemes to deal with the obstacles. The main idea is to pay penalize of the obstacles in the calculation of distance between each pair of sites. For example, the original shortest distance from site *i* to site *j* is their Euclidean distance *d*(*i*, *j*). Now with an obstacle between sites *i* and *j*, we use a new shortest distance $d'(i,j)$ that reflects the influence of such an obstacle is constructed. Then TSP algorithm can be adopted to calculate a new trajectory. For the adjustment of the trajectory, if the trajectory after adjustment meets an obstacle, we use the following method to re-calculate the new collection center. An example is illustrated in Fig. 5 that handles an obstacle in case 1. With the obstacle, the original trajectory in Fig. 5(a) is not feasible. Then we start from $p_{i-1}$ and $p_{j+1}$, each of which generates two rays that are both tangent with the obstacle. The four rays form an infeasible region as shown in Fig. 5(b), in which the new collection center cannot identify. Then we check if there is any feasible arc in the communication disk that the optimal new collection center $p_j^*$ can identify. For case 2 and case 3, similar methods can be adopted.

### C. Distributed Data Generation Rate and Link Flow Rate Optimization

*1) Formalization of a Convex Optimization Problem:* Given the energy allocation solution ***a***(*t*), the aggregation node set $\mathcal{A}(t)$ and the data collection trajectory in time period *t*, we propose a distributed algorithm to maximize the network utility, by optimizing the data generation rate of each sensor and the data flow rate of each link in the network.

As described in the network flow model, a sensor node can distribute its generated sensory data with relayed data to its neighbors and determines to which aggregation node(s) the outgoing data flows. While the MS is moving along its planned trajectory, the virtual aggregation nodes in $\mathcal{W}(t)$ can transmit their data to the passing by MS directly without influencing its speed. By adopting this strategy, the network utility can be potentially improved since these data flows are supposed to be delivered through multi-hops to aggregation nodes then to the MS. In other words, the energy cost for intermediate relays decreases. We use $\mathcal{S}(t)$ to indicate path segments formed by the intersection points of the communication circles with the traveling path, where each segment is consist of two successive intersection points.

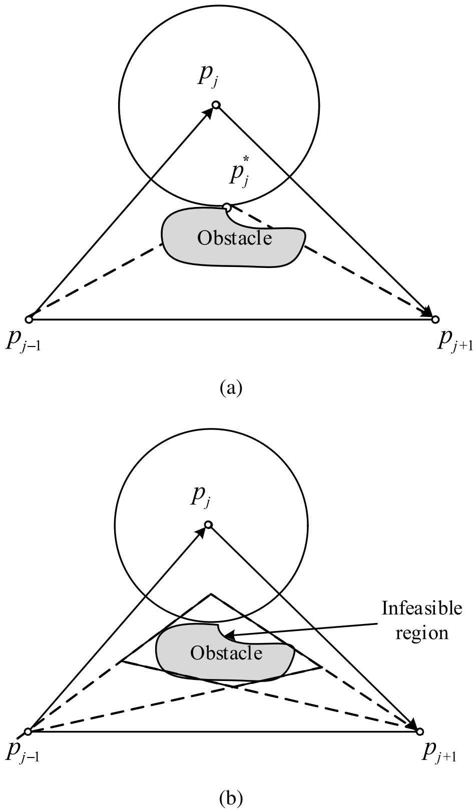


Fig. 5. Handling obstacle when planning the trajectory for the MS.

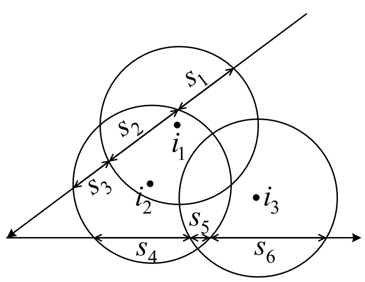


Fig. 6. The straight line with arrow is part of the trajectory.

An example is given in Fig. 6 to illustrate our model, where $\mathcal{W}(t) = \{i_1, i_2, i_3\}$ and $\mathcal{S}(t) = \{s_1, s_2, \ldots, s_6\}$. To reflect this in the network model, we treat each path segment as a dummy node, then expand the network graph by adding a directional link (*i*, *s*) for each $i \in \mathcal{W}(t)$ and each $s \in \mathcal{S}(t)$, i.e., we have $\mathcal{O}_{i_2} = \{s_2, s_3, s_4, s_5\}$ in the figure. Since the MS can receive data from at most one sensor at one time under the half-duplex model, as long as the sum of transmission time durations from each node $i \in \mathcal{W}(t)$ to each $s \in \mathcal{S}(t)$, denoted $\tau_{is}(t)$, does not exceed the maximum sojourn time of the MS traveling along path segment *s*, i.e., the maximum reception duration of the MS within *s*, there always exists a feasible non-collision transmission scheduling for each related node *i*, which means the following should be satisfied:

$$\sum_{i:s\in\mathcal{O}_i} \tau_{is}(t) \le \frac{|s|}{v}, \ \forall s \in \mathcal{S}(t), \tag{22}$$

where $|s|$ denotes the path length of *s* and *v* is the traveling velocity of the MS. For the sake of consistency, we write constraint (22) in the form of flow rate. In fact, the equivalent flow rate for link $(i, s)|_{i\in\mathcal{W}(t), s\in\mathcal{S}(t)}$ in each time period is $f_{is}(t) := \frac{\pi_{\mathrm{i}}\tau_{is}(t)}{T}$, where $\pi_i$ is the data transmission rate of *i*. Then we reformulate inequality (22) as:

$$\sum_{i:s\in\mathcal{O}_i} f_{is}(t) \le \frac{|s|}{v} \cdot \frac{\pi_i}{T}, \ \forall s \in \mathcal{S}(t), \tag{23}$$

The optimization problem then determines the source rates of sensors and the flow rates over links to maximize then network utility, given the energy budget and data collection trajectory in time period *t*. We formulate the problem as

$$\textbf{P3}: \max_{\boldsymbol{r}(t),\boldsymbol{f}(t)} \ \sum_{i\in\mathcal{N}} \log(r_i(t)), \tag{24}$$

$$\text{subject to Constraints (6), (7)}$$

$$c_i(t) \le \frac{a_i(t)}{T}, \ \forall i \in \mathcal{N}, \tag{25}$$

$$\sum_{l\in\mathcal{I}_s(t)} f_l(t) \le \frac{|s|}{v} \cdot \frac{\pi_u}{T}, \ u = \overleftarrow{l}, \ \forall s \in \mathcal{S}(t), \tag{26}$$

$$r_s(t) = 0, \ \forall s \in \mathcal{S}(t). \tag{27}$$

In constraint (26), we define $u := \overleftarrow{l}$ for a link $l := (u,\, s)$. Inequality (25) is the energy budget constraint for each sensor. For each of sensors, the energy consumption cannot exceed its allocated energy in each time period in order to keep energy neutral. Constraint (26) follows inequality (23) which is necessary to achieve collision-free data transmission from virtual aggregation nodes to the moving sink. And constraint (27) holds for the reason that an MS does not generate sensory data by itself.

*2) ADMM-Based Distributed Algorithm:* The rest it to tackle problem P3, we adopt a distributed version of ADMM [26], [28], which can outperform the dual decomposition (DD) based methods in the convergence speed and suitable for large-scale optimization problems.

The difficulty to tackle problem P3 in a distributed manner lies in the two-sidedness of the flow rate to optimize over each link, which belongs to an outgoing link and an incoming link for two sensor nodes. To decompose P3 with appropriately handling this coupling, we introduce a local copy of the global flow rate for each sensor *i*, which reflects the global flow rates over *i*'s neighboring links in node *i*'s view. Specifically, we introduce local variables $\widehat{f}_l^i$ to represent the flow rate $f_l$ in sensor *i*'s view, where *l* is a link associated with node *i*. For a link $l := (i, j)$, we define $i := \overleftarrow{l}$ and $j := \overrightarrow{l}$. Note that we omit the suffix (*t*) in the expressions for the sake of simplicity, e.g., we use $f_l$ to represent $f_l(t)$. We define local link flow rate vectors for each sensor *i* as $\widehat{\boldsymbol{f}}_i := \{\widehat{f}_l^i \mid l \in \mathcal{L}_i\}$. Let $\mathcal{L}_i := \mathcal{O}_i \cup \mathcal{I}_i$. Then, we reformulate the relaxed version of P3 as follows.

$$\textbf{P4}: \min_{\boldsymbol{r},\boldsymbol{f},\widehat{\boldsymbol{f}}} \ -\sum_{i\in\mathcal{N}} \log(r_i), \tag{28}$$

$$\text{subject to } \left(r_i, \widetilde{\boldsymbol{f}}_i\right) \in \mathcal{V}_i, \ \forall i \in \mathcal{N}\cup\mathcal{S}, \tag{29}$$

$$\widehat{f}_l^i = f_l, \ \forall i \in \mathcal{N}\cup\mathcal{S}, \forall l \in \mathcal{L}_i, \tag{30}$$

where $\mathcal{V}_i$ is the convex set of feasible solutions defined by:

$$\mathcal{V}_i := \Bigg\{ (r_i, \tilde{\boldsymbol{f}}_i) \mid \sum_{l\in\mathcal{O}_i} \widehat{f}_l - \sum_{m\in\mathcal{I}_i} \widehat{f}_m = r_i, \sum_{l\in\mathcal{O}_i} e^{tx}\widehat{f}_l + \sum_{m\in\mathcal{I}_i} e^{rx}\widehat{f}_m + e^s r_i \le a_i^*/T, \sum_{l\in\mathcal{L}_i} \frac{\widehat{f}_l}{\pi_l} \le 1, \left(r_i, \tilde{\boldsymbol{f}}_i\right) \succeq 0. \Bigg\}, \forall i \in \mathcal{N} \tag{31}$$

and

$$\mathcal{V}_i := \Bigg\{ (r_i, \tilde{\boldsymbol{f}}_i) \mid \sum_{l\in\mathcal{O}_i} \widehat{f}_l = \sum_{m\in\mathcal{I}_i} \widehat{f}_m, \sum_{l\in\mathcal{I}_i} \widehat{f}_l \le \frac{|i|}{v}\cdot\frac{\pi_i}{T}, \ r_i = 0, \ \tilde{\boldsymbol{f}}_i \succeq 0. \Bigg\}, \forall i \in \mathcal{S}, \tag{32}$$

In order to make problem P4 suitable for the ADMM, we define the indicator function of $\mathcal{V}_i$ denoted by $\mathcal{I}_i$:

$$\mathcal{I}_i\left(r_i, \tilde{\boldsymbol{f}}_i\right) := \begin{cases} 0, & \text{if } \left(r_i, \tilde{\boldsymbol{f}}_i\right) \in \mathcal{V}_i \\ +\infty, & \text{otherwise.} \end{cases} \tag{33}$$

Then, an equivalent formulation of P4 is defined as follows.

$$\begin{aligned} \mathbf{P5}:\ & \min_{\boldsymbol{r},\boldsymbol{f},\widehat{\boldsymbol{f}}} \sum_{i\in\mathcal{N}} \left( -\log(r_i) + \mathcal{I}_i\left(r_i, \tilde{\boldsymbol{f}}_i\right)\right), \\ & \text{subject to constraint (30).} \end{aligned} \tag{34}$$

To solve problem P5, we first form an augmented Lagrangian for the objective function as:

$$\mathfrak{L}(\boldsymbol{r}, \boldsymbol{f}, \widehat{\boldsymbol{f}}, \boldsymbol{\lambda}) = \sum_{i\in\mathcal{N}} \left( -\log(r_i) + \mathcal{I}_i(r_i, \tilde{\boldsymbol{f}}_i)\right) + \sum_{i\in\mathcal{N}} \left( \sum_{l\in\mathcal{L}_i} \lambda_l^i \left(\widehat{f}_l^i - f_l\right) + \frac{\rho}{2} \sum_{l\in\mathcal{L}_i} \left(\widehat{f}_l^i - f_l\right)^2 \right) \tag{35}$$

where $\boldsymbol{\lambda} := \{\lambda_l^i \mid i \in \mathcal{N}, l \in \mathcal{L}_i\}$ are the introduced Lagrange multipliers for each sensor node and $\rho > 0$ is a penalty parameter for adjusting the convergence speed of the algorithm of ADMM.

The proposed algorithm proceeds iteratively to update the optimization value and lagrange variables as follows.

$$\left(r_i[m], \tilde{\boldsymbol{f}}_i[m]\right) = \arg\min_{(r_i, \tilde{\boldsymbol{f}}_i)} \Bigg\{ -\log(r_i) + \mathcal{I}_i\left(r_i, \tilde{\boldsymbol{f}}_i\right) + \sum_{l\in\mathcal{L}_i} \lambda_l^i \left(\widehat{f}_l^i - f_l[m-1]\right) + \frac{\rho}{2} \sum_{l\in\mathcal{L}_i} (\widehat{f}_l^i - f_l[m-1])^2 \Bigg\}, \forall i \in \mathcal{N}, \tag{36}$$

$$\boldsymbol{f}[m] = \arg\min_{\boldsymbol{f}} \Bigg\{ \sum_{i\in\mathcal{N}} \left( \sum_{l\in\mathcal{L}_i} \lambda_l^i \left(\widehat{f}_l^i[m] - f_l\right) + \frac{\rho}{2} \sum_{l\in\mathcal{L}_i} \left(\widehat{f}_l^i[m] - f_l\right)^2 \right) \Bigg\}, \tag{37}$$

$$\lambda_l^i[m] = \lambda_l^i[m] + \rho\left(\widehat{f}_l^i[m] - f_l^i[m]\right), \quad \forall i \in \mathcal{N}, \forall l \in \mathcal{L}_i, \tag{38}$$

where the suffix $[m]$ denotes the iteration index.

In the first step, with given global flow rates $\boldsymbol{f}$, we aim to optimize the local flow rates $\widehat{\boldsymbol{f}}_{\boldsymbol{i}}$ and source rate $r_i$ for each node $i \in \mathcal{N}$, while in the second step we keep $\widehat{\boldsymbol{f}}$ fixed to optimize the global flow rate $\boldsymbol{f}$. The associated lagrange multipliers $\boldsymbol{\lambda}$ are updated in the third step. This iterative method enables the decomposition of the ADMM while guaranteing its convergence property [28].

The first step (36) solves the following equivalent problem:

$$\begin{aligned} \min_{(r_i, \tilde{\boldsymbol{f}}_i)} & \left\{ -\log(r_i) + \left( \sum_{l\in\mathcal{L}_i} \lambda_l^i \widehat{f}_l^i + \frac{\rho}{2} \sum_{l\in\mathcal{L}_i} \left(\widehat{f}_l^i - f_l[m-1]\right)^2 \right) \right\} \\ \text{subject to} & \ \left(r_i, \tilde{\boldsymbol{f}}_i\right) \in \mathcal{V}_i, \end{aligned} \tag{39}$$

for each sensor $i$, which is a convex optimization problem and can be solved efficiently by existing interior-point methods.

Since the second step involves a global optimization, we focus on its decomposition. The key idea is to transform the node-specific constraint to the link-specific constraint, based on which, we rewrite the summation notation $\sum_{i\in\mathcal{N}}\sum_{l\in\mathcal{L}_i}$ as $\sum_{l\in\mathcal{E}}\sum_{i\in\overleftarrow{l}\cup\overrightarrow{l}}$, which separates (37) into the following subproblems for each link $l$:

$$\boldsymbol{f}_l[m+1] = \arg\min_{\boldsymbol{f}_l} \left( -\lambda_l^{\overleftarrow{l}}[m] f_l + \frac{\rho}{2}\left(\widehat{f}_l^{\overleftarrow{l}}[m] - f_l\right)^2 - \lambda_l^{\overrightarrow{l}}[m] f_l + \frac{\rho}{2}\left(\widehat{f}_l^{\overrightarrow{l}}[m] - f_l\right)^2 \right), \ \forall l \in \mathcal{E}. \tag{40}$$

Note that the objective function $\boldsymbol{f}_l[m+1]$ defined in (40) is strictly convex due to the added augmented lagrangians. Thus, there exists a unique optimal solution for $\boldsymbol{f}_l$, where we let the derivatives of (40) to be zero and obtain:

$$f_l[m+1] = \frac{1}{2}\left(\widehat{f}_l^{\overleftarrow{l}}[m] + \widehat{f}_l^{\overrightarrow{l}}[m]\right) + \frac{1}{2\rho}\left(\lambda_l^{\overleftarrow{l}}[m] + \lambda_l^{\overrightarrow{l}}[m]\right), \forall l \in \mathcal{E}. \tag{41}$$

We require each node $i \in \mathcal{N}$ to calculate Eq. (41) distributedly, while exchanging necessary local variables with their neighbors to update global flow rates. Since nodes in $\mathcal{S}$ are virtualized , we adopt a work-around by using a connected set of sensor nodes to simulate each virtual node $s \in \mathcal{S}$, which satisfies the following conditions. First, each node connecting $s$ should be connected to the set. Also, the values of associated variables among the nodes in the connected set should keep consistent with each other, in order to make optimization variables *local*. And third, the size of the set should be small to keep the low communication overhead. A simple scheme is adopted here to obtain a feasible set for each $s$. For each pair of nodes that are connected to $s$, find the shortest path between them and record the nodes along the path, and we make a union-operation to all recorded nodes to obtain an equivalent set for $s$.

Finally, in the third step (41), the dual variables associated with each sensor are updated. $\rho$ represents the step size and influences convergence speed and precision of ADMM,

**Algorithm 1** The Distributed Utility Maximization Algorithm

$r_i = 0$ for any $i \in \mathcal{N}$
$f_l[0] = 0$ for any $l \in \mathcal{L}$
**for** each sensor node $i \in \mathcal{N} \cup \mathcal{S}$ **do**
  Iteration index $m = 1$
  Solve the convex problem (39), obtain data generation rate $r_i$ and local link flow rate vector $\tilde{\boldsymbol{f}}_i$
  **for** each link $l$ associated with $i$ **do**
    Update the global link flow rate $f_l[m]$ according to Eq. (41)
    $m = m + 1$
  **end for**
**end for**

the optimal value of which is chosen by practical simulations. The pseudo-code of the distributed algorithm is given in Algorithm 1.

*3) A Heuristic Algorithm:* The computational overhead of Algorithm 1 can sometimes be heavy for resource constrained sensor nodes. The reason is that the data collection trajectory may intersects frequently with the communication disks of sensor nodes, especially when the network is dense. As a result, the number of V2MS links can significantly increases, which causes much overheads for sensors to execute the iterative algorithms for all their associated links. Therefore, we develop a fast heuristic algorithm to optimize data generation and link rates. We first maximize the utility in terms of data flow rates of V2MS links, then optimize the data flow rates of all the other links and data generation rates of sensors. Since these coupled links and the corresponding constraints are separately optimized, the computing overhead can be reduced and the convergence speed can be accelerated. Based on the experimental results, we find that the communication time window for the virtual aggregation nodes to the moving sink is limited compared to the stop time of the MS at collection sites in each time period. Thus, the benefit of enabling data transfer from virtual aggregation nodes to the moving sink is controllable, and this does not strongly influence the optimization of data flow rates of S2S and V2MS links.

### D. Time Complexity Analysis

We analyze the complexity performance of the proposed algorithms as follows. The proposed MDG-EH algorithm is composed of three sub-algorithms: a harvested energy budget allocation sub-algorithm, an MS trajectory planning sub-algorithm and a data flow optimization sub-algorithm. For the first sub-algorithm, which contains a quadratic program P2 with linear constraints. The worst-case time complexity is $O(X^3)$ for each sensor node *i*, where *X* represents the sum of the number of variables in the standard formula. And since *X* is linear with the sum of the number of variables in P2, which is *K*, the time complexity of the algorithm for P2 is $O(K^3)$. For the second sub-algorithm, it contains finding a series of TSPs and trajectory adjustment steps. In each TSP and adjustment step, as the TSP is NP-Complete problem, it is unlikely to have an optimization algorithm which can solve this particular problem in polynomial time in the worst case. Instead, a polynomial-time approximation algorithm is adopted. And all adjustment steps can be done in polynomial time. The time complexity of solving the second sub-problem is $O(P(1)) + O(P(2)) + \; + O(P(u))$, where $P(\cdot)$ is a polynomial function, *u* is the total number of iterations of the second sub-problem. For the third sub-algorithm, Algorithm 1 contains a convex optimization problem (39) and a loop. For the convex optimization problem (39), the worst-case time complexity is $O(Y^3)$ for each sensor node *i*, where $Y = |\mathcal{L}_i| + 1$. And the loop contains $|\mathcal{L}_i|$ steps in total. Therefore, the time complexity of the third sub-algorithm is $O(Y^3) + O(|\mathcal{L}_i|) = O(Y^3)$.

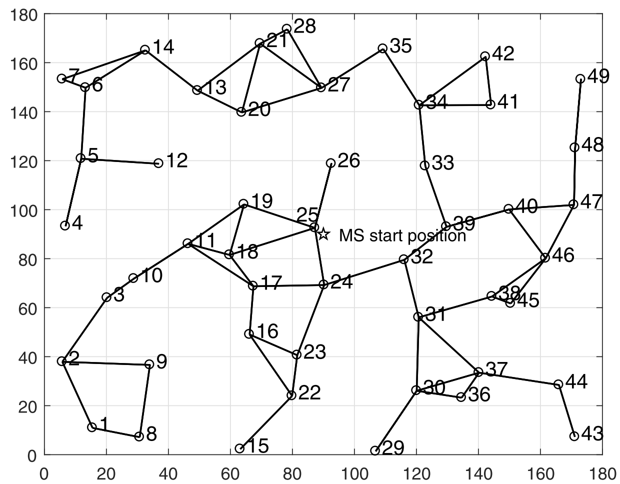


Fig. 7. Network topology with 49 sensor nodes, where the star labels the starting position of the MS.

TABLE I
PARTIAL PARAMETER VALUES

| Parameter | value | Parameter | value |
|---|---|---|---|
| $e^{tx}$ | 0.24mJ | $l_b$ | 6000m |
| $e^{rx}$ | 0.24mJ | $v$ | 1m/s |
| $e^s$ | 0.002J | $b_i^n$ | $B/2$ |
| $T$ | 1h | $K$ | 12 |
| $A_{sp}$ | 1cm$^2$ | $\eta$ | 0.1 |
| $B$ | 108J | $b_i^n$ | $B/2$ |

## V. PERFORMANCE EVALUATION

In this section, numerical results are demonstrated through extensive simulations in MATLAB to provide readers details and insights of our proposed schemes for mobile data collection with energy harvesting sensors. We adopt a randomly generated network topology of $|\mathcal{N}| = 49$ nodes in a 180m $\times$ 180m squared area, where sensors are deployed uniformly in the area, as depicted in Fig. 7. The maximum communication range of each sensor *R* is set to 30m, and the lines between sensor nodes in the topology represents the links in the static network. Each sensor is equipped with a half-duplex transceiver like CC2500 [29] and a solar collector, the values of detailed network parameters are provided

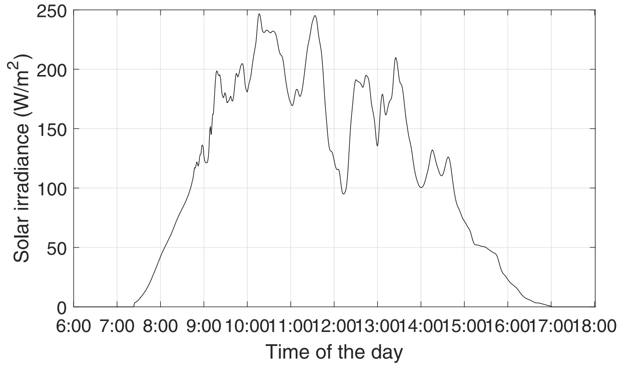


Fig. 8. Experiment solar profile from 6:00 to 18:00 in Jan. 15th, 2017.

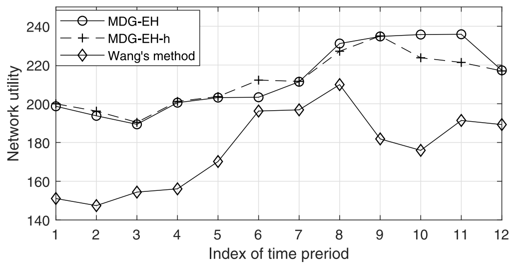


Fig. 9. Network utility achieved at each time period.

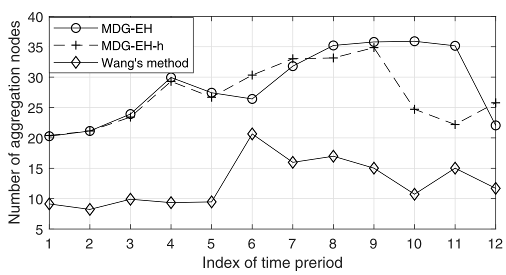


Fig. 10. Number of aggregation nodes selected at each time period.

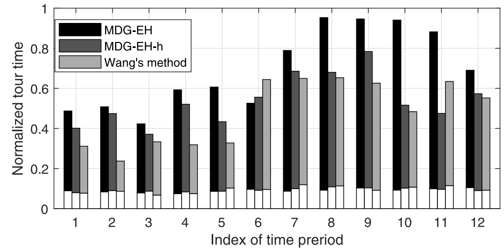


Fig. 11. Normalized data collection trajectory time of the MS within each time period.

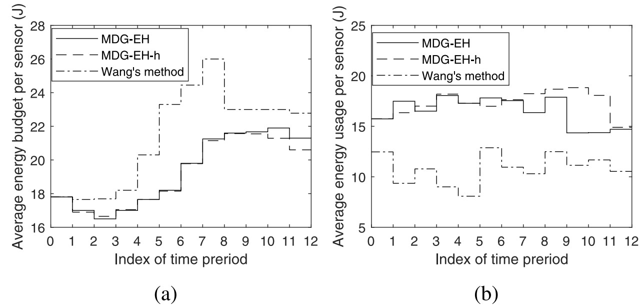


Fig. 12. Average energy allocation and energy usage for sensors at each time period. (a)Average energy allocation. (b)Average energy usage.

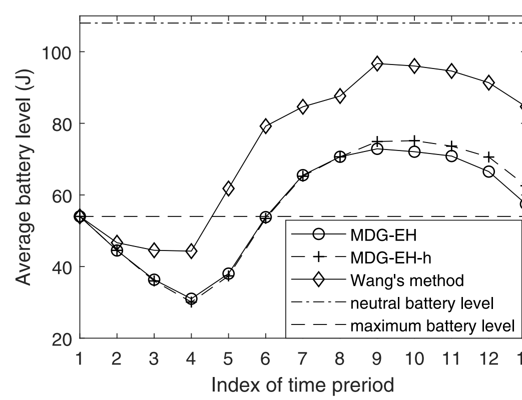


Fig. 13. Average battery level at the start of each time period.

in Table I. $A_{sp}$ represents the solar panel area and $\eta$ is the energy transform efficiency. Fig. 8 presents a 1-day solar profile obtained from the baseline measurement system (BMS) of NREL solar radiation research laboratory [32]. The solar profile for analysis is tailored from 6:00 am to 6:00 pm. Since we set $T = 1h$, the whole period we study on consists of 12 intervals. The following algorithms are examined and compared in the simulation:

- MDG-EH: proposed mobile data gathering algorithm for EH-WSNs, including three dynamic sub-programs.
- MDG-EH-h: a heuristic version of proposed mobile data gathering algorithm, where the rate optimization of sensors to the moving MS is simplified in the third sub-program, in order to reduce iteration and communication overhead.
- Wang's method: an optimization framework proposed by Wang *et al.* [12], where the MS must traverse each of the aggregation nodes in order to collect data from them. We add the proposed balanced energy budget pre-allocation scheme to Wang's method in order to make a fair comparison against our proposed algorithms.

## A. Performance Analysis Across the Whole Period

To reflect the dynamics on the conditions and our proposed strategies, we first demonstrate the performance over the whole period. We are interested in the following indicators of the network over time: the allocation of harvested energy for sensors, the battery level of sensors, the achieved utility of the network, etc. Fig. 9 depicts the results of utilities achieved by the three mentioned algorithms at each time period. It can be seen that with proposed variance-minimal energy allocation strategy, all the three algorithms achieve the balanced network performance under the nonuniform solar power provided. MDG-EH achieves the highest utility over time while MDG-EH-h achieves comparable performance, both of which outperform Wang's method. The reason can be found from Fig. 10, which depicts the number of aggregation nodes selected by each algorithm at each time period, sharing the same trend with the utility changes in Fig. 9. With neighborhood traveling adopted, MDG-EH and MDG-EH-h are able to select more aggregation nodes under given the trajectory

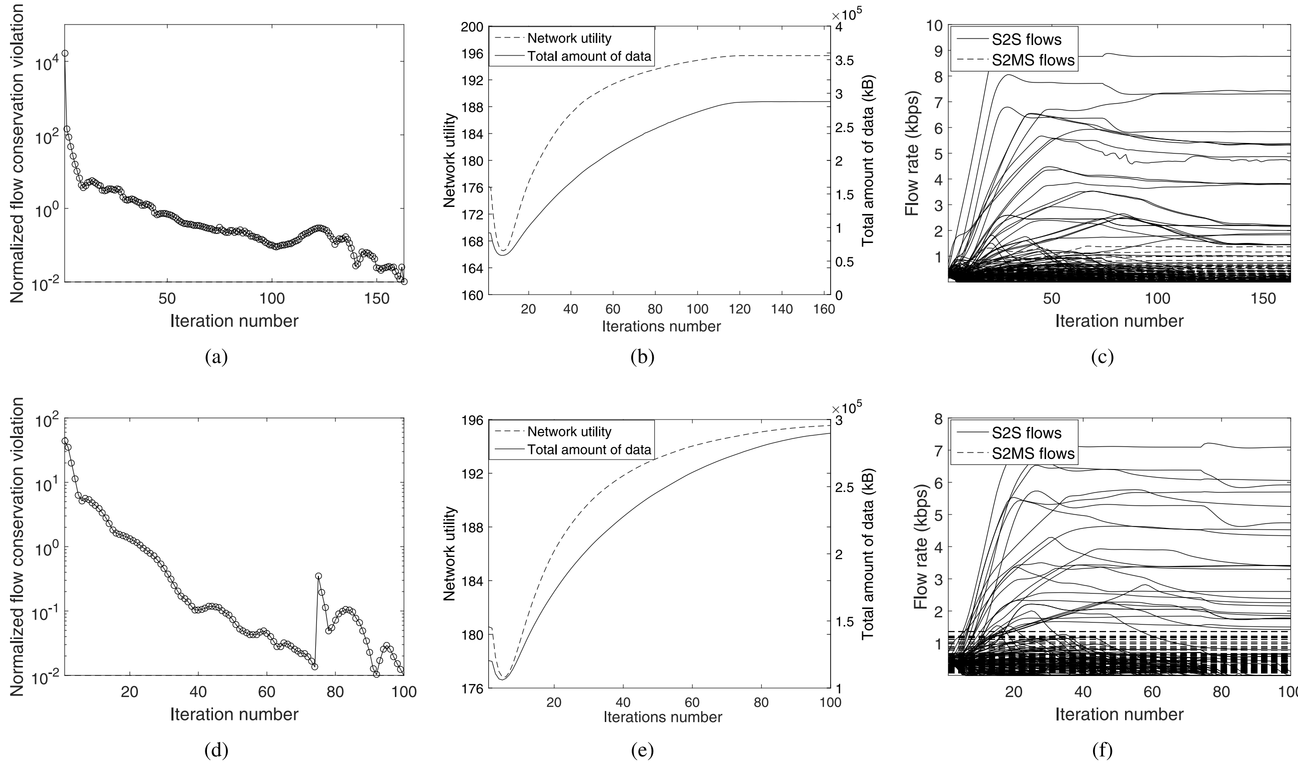


Fig. 14. Convergence of normalized flow conservation violation, of network utility and of flow rates for MDG-EH and MDG-EH-h, respectively. (a), (b) and (c) are for MDG-EH-h, (d), (e) and (f) are for MDG-EH-h.

length bound, and since the increase on the number of aggregation nodes leads to the decrease in the total energy cost to deliver per unit of data to the MS, as a result, the network performance can be improved.

Fig. 11 depicts the normalized trajectory time of the MS verses time period index, where the normalized trajectory time is defined as the sum of the moving time and the sojourn time of the MS divided by the length of one time period. The white bars in the figure indicates the moving time of the MS for each algorithm at the associated intervals. We can conclude that, first, the time spent on gathering data is much longer than that spent on moving for an MS. Second, MDG-EH-h cost less time than MDG-EH, which means that it achieves lower delay in mobile data gathering. And third, the distribution of the trajectory time verifies the necessariness of the proposed balanced energy allocation strategy. Otherwise, for example, a harvest-then-exhaust energy strategy is adopted, almost certainly the trajectory time of the MS exceeds the time duration length.

Fig. 12 shows the average energy allocation and average energy consumption for sensors during each time period by different algorithms. We can find that the amount of energy used by sensors is not necessarily related to the amount of energy allocated to sensors, since the allocated energy may not be fully utilized by the sensors. And there exists a rising stage in the energy allocation for the three comparison algorithms, which means that the unutilized energy in one period is added up to the allocatable energy for the subsequent intervals. It also can be found that the average energy usage, to some extent, reflect the utility that can be achieved. Clearly, MDG-EH and MDG-EH-h achieve both higher energy usage and energy usage ratio than that of Wang's method.

To examine whether energy neutral is maintained in the network, we record the average battery level (ABL) of sensors in the beginning of each time period, as illustrated in Fig. 13. Two indicators are investigated: first, we check whether the average battery level returns the initial battery level at the end of $K$ periods. Second, we average the values of ABL over the $K$ intervals and compare with $b_n$ to check how close we are to the energy neutral level in the whole period. From the result, it can be observed that MDG-EH basically achieves battery neutralization without violating battery capacity constraint, and MDG-EH-h is close to the neutral line. Both of them outperform Wang's method.

## B. Performance Analysis Within One Period

We analyze the convergence behavior of the proposed algorithms within one time period. We select the first period, for demonstration purpose, to make a comparison between MDG-EH and MDG-EH-h. Fig. 14(a)$\sim$(c) illustrates the convergence of normalized flow conservation violation, of network utility and flow rates for MDG-EH, respectively. Similarly, Fig. 14(e)$\sim$(f) demonstrate the corresponding convergence behaviors of MDG-EH-h. As can be seen in Fig. 14, both of the algorithms converge to the defined stopping criterion within dozens of iterations, making them feasible algorithms. With similar network utility achieved and similar total amount of data gathered, MDG-EH-h converges faster than MDG-EH by 62%. The reason is that in MDG-EH-h, the flow rates to

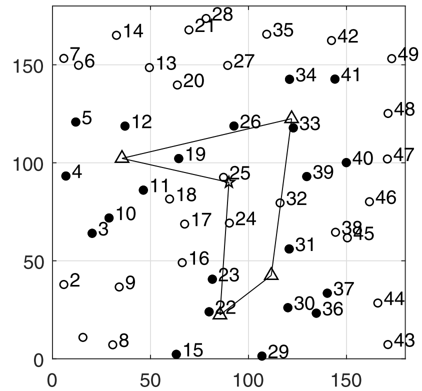

(a)

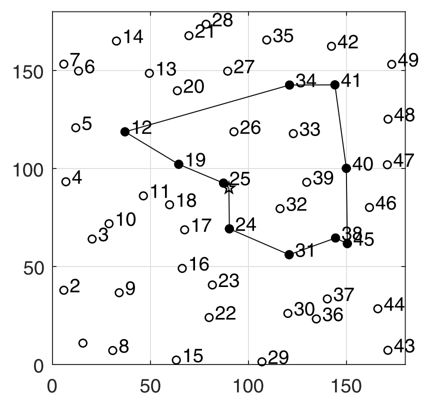

(b)

Fig. 15. The data collection trajectory of the MS generated by (a)MDG-EH. (b)Wang's method.

the moving MS is determined beforehand, the decrease in the number of optimization variables accelerates the optimization process. Considering the number of virtual nodes generated by MDG-EH (57), the overall computational overhead of MDG-EH-h is even less compared to MDG-EH.

In Fig. 14(c) and (f), the iterative behavior of flow rates within sensors (S2S flows), and of sensors to the moving MS (S2MS flows) for two algorithms are represented. As can be observed, the S2MS flow rates is much lower compared with the S2S flow rates, since the capacity of each virtual node (related to the length of each trajectory segment) is limited. Compared with Fig. 11, it can be concluded that the proposed data transmission strategy can reduce the data collection delay significantly.

The data collection trajectories of the MS delivered by the proposed algorithm MDG-EH and the benchmark algorithm are plotted in Fig. 15. Note that the algorithms MDG-EH and MDG-EH-h share the same trajectory but differentiate themselves in network data flow rate optimization schemes, therefore, we plot one trajectory for the proposed two algorithms for comparison purpose. In Fig. 15, black nodes represent dedicated aggregation nodes. Triangles in Fig. 15(a) represent collection centers where the MS stops to collect data from these dedicated aggregation nodes. In Fig. 15(b), however, the MS has to traverse the exact position of each aggregation node. As a result, with the same trajectory length

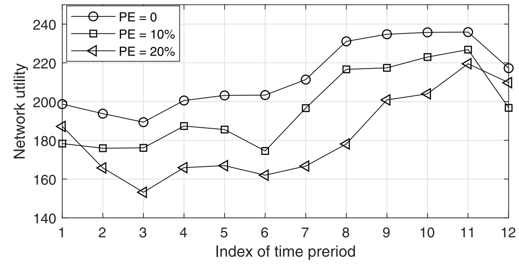


Fig. 16. Influence of harvested energy prediction error over time periods.

constraint, the proposed trajectory planning algorithm can deliver more aggregation nodes, therefore, can achieve better network performance with the limited energy budget and given trajectory length constraint.

### C. Impact of Prediction Error

The rest is to investigate the impact of prediction errors on the energy harvesting rate. First, from the aspect of mitigating such prediction errors, we could adopt a more accurate prediction model. Specifically for solar and wind energy prediction, recent studies proposed several enhanced models such as a combined short-term and long-term prediction model [24] that can achieve more reliable estimation results. Second, since an overestimation could cause the decline on the network performance, we focus mainly on the overestimation of harvested energy. We pre-allocate the energy budget for each sensor, which is overestimated, then energy shortage occurs and only harvested energy is not enough for each node to relay/transmit all data to the mobile sink. As a result, network performance will decrease since some data cannot be delivered to the sink and is dropped. We evaluate the impact of average prediction error (PE) of overestimation in Fig. 16. As can be observed, compared to the case that PE=0, the average network performance decrease is 8.1% and 15.3%, respectively when PE=10% and PE=20%.

## VI. Conclusion

In this paper, we first proposed an optimization framework for data collection in EH-WSNs via an MS, then developed a dynamic optimization algorithm to find the data collection trajectory for the MS, and determine data flow rates among sensors to achieve long-term network utility maximization and energy neutrality. The proposed algorithms include a balanced energy budget management for sensors, an efficient mechanism to identify aggregation nodes, a method to progressively reduce the length of the data collection trajectory, and a distributed algorithm that enables each sensor to determine its optimal data generation rate and associated link flow rates with the planned mobile collection trajectory. Finally we conducted numerical experiments to evaluate the performance of the proposed algorithms, which show the effectiveness of the proposed algorithms.

## References

[1] X. Liu, H. Zhao, X. Yang, and X. Li, "SinkTrail: A proactive data reporting protocol for wireless sensor networks," *IEEE Trans. Comput.*, vol. 62, no. 1, pp. 151–162, Jan. 2013.

[2] S. Olariu and I. Stojmenovic, "Design guidelines for maximizing lifetime and avoiding energy holes in sensor networks with uniform distribution and uniform reporting," in *Proc. IEEE INFOCOM*, Barcelona, Spain, 2006, pp. 1–12.

[3] M- L. Ku, W. Li, Y. Chen, and K. J. R. Liu, "Advances in energy harvesting communications: Past, present, and future challenges," *IEEE Commun. Surveys Tuts.*, vol. 18, no. 2, pp. 1384–1412, 2nd Quart., 2016.

[4] X. Ren, W. Liang, and W. Xu, "Data collection maximization in renewable sensor networks via time-slot scheduling," *IEEE Trans. Comput.*, vol. 64, no. 7, pp. 1870–1883, Jul. 2015.

[5] A. Mehrabi and K. Kim, "Maximizing data collection throughput on a path in energy harvesting sensor networks using a mobile sink," *IEEE Trans. Mobile Comput.*, vol. 15, no. 3, pp. 690–704, Mar. 2016.

[6] R. Deng, Y. Zhang, S. He, J. Chen, and X. Shen, "Maximizing network utility of rechargeable sensor networks with spatiotemporally coupled constraints," *IEEE J. Sel. Areas Commun.*, vol. 34, no. 5, pp. 1307–1319, May 2016.

[7] Y. Zhang, S. He, and J. Chen, "Near optimal data gathering in rechargeable sensor networks with a mobile sink," *IEEE Trans. Mobile Comput.*, vol. 16, no. 6, pp. 1718–1729, Jun. 2017.

[8] S. Guo, C. Wang, and Y. Yang, "Joint mobile data gathering and energy provisioning in wireless rechargeable sensor networks," *IEEE Trans. Mobile Comput.*, vol. 13, no. 12, pp. 2836–2852, Dec. 2014.

[9] A. Dumitrescu and J. S. B. Mitchell, "Approximation algorithms for TSP with neighborhoods in the plane," *J. Algorithms*, vol. 48, no. 1, pp. 135–159, 2003.

[10] L. He, J. Pan, and J. Xu, "A progressive approach to reducing data collection latency in wireless sensor networks with mobile elements," *IEEE Trans. Mobile Comput.*, vol. 12, no. 7, pp. 1308–1320, Jul. 2013.

[11] C.-F. Cheng and C.-F. Yu, "Data gathering in wireless sensor networks: A combine–TSP–reduce approach," *IEEE Trans. Veh. Technol.*, vol. 65, no. 4, pp. 2309–2324, Apr. 2016.

[12] C. Wang, S. Guo, and Y. Yang, "An optimization framework for mobile data collection in energy-harvesting wireless sensor networks," *IEEE Trans. Mobile Comput.*, vol. 15, no. 12, pp. 2969–2986, Dec. 2016.

[13] Y. Zhang, S. He, J. Chen, Y. Sun, and X. S. Shen, "Distributed sampling rate control for rechargeable sensor nodes with limited battery capacity," *IEEE Trans. Wireless Commun.*, vol. 12, no. 6, pp. 3096–3106, Jun. 2013.

[14] S. Chen, P. Sinha, N. B. Shroff, and C. Joo, "A simple asymptotically optimal joint energy allocation and routing scheme in rechargeable sensor networks," *IEEE/ACM Trans. Netw.*, vol. 22, no. 4, pp. 1325–1336, Aug. 2014.

[15] R.-S. Liu, P. Sinha, and C. E. Koksal, "Joint energy management and resource allocation in rechargeable sensor networks," in *Proc. IEEE INFOCOM*, San Diego, CA, USA, 2010, pp. 1–9.

[16] L. Lin, N. B. Shroff, and R. Srikant, "Asymptotically optimal energy-aware routing for multihop wireless networks with renewable energy sources," *IEEE/ACM Trans. Netw.*, vol. 15, no. 5, pp. 1021–1034, Oct. 2007.

[17] Y. Zhang, S. He, and J. Chen, "Data gathering optimization by dynamic sensing and routing in rechargeable sensor networks," *IEEE/ACM Trans. Netw.*, vol. 24, no. 3, pp. 1632–1646, Jun. 2016.

[18] F. A. Aoudia, M. Gautier, and O. Berder, "Distributed computation of fair packet rates in energy harvesting wireless sensor networks," *IEEE Wireless Commun. Lett.*, vol. 6, no. 5, pp. 626–629, Oct. 2017.

[19] S. Yang and J. A. McCann, "Distributed optimal lexicographic max-min rate allocation in solar-powered wireless sensor networks," *ACM Trans. Sensor Netw.*, vol. 11, no. 1, p. 9, 2014.

[20] M. Zhao, J. Li, and Y. Yang, "A framework of joint mobile energy replenishment and data gathering in wireless rechargeable sensor networks," *IEEE Trans. Mobile Comput.*, vol. 13, no. 12, pp. 2689–2705, Dec. 2014.

[21] C. Zhan, Y. Zeng, and R. Zhang, "Energy-efficient data collection in UAV enabled wireless sensor network," *IEEE Wireless Commun. Lett.*, vol. 7, no. 3, pp. 328–331, Jun. 2018.

[22] Y. Zeng and R. Zhang, "Energy-efficient UAV communication with trajectory optimization," *IEEE Trans. Wireless Commun.*, vol. 16, no. 6, pp. 3747–3760, Jun. 2017.

[23] D.-T. Ho, E. I. Grøtli, P. B. Sujit, T. A. Johansen, and J. B. Sousa, "Optimization of wireless sensor network and UAV data acquisition," *J. Intell. Robot. Syst.*, vol. 78, no. 1, pp. 159–179, 2015.

[24] A. Cammarano, C. Petrioli, and D. Spenza, "Online energy harvesting prediction in environmentally powered wireless sensor networks," *IEEE Sensors J.*, vol. 16, no. 17, pp. 6793–6804, Sep. 2016.

[25] Y. Ye and E. Tse, "An extension of Karmarkar's projective algorithm for convex quadratic programming," *Math. Program.*, vol. 44, nos. 1–3, pp. 157–179, 1989.

[26] M. Leinonen, M. Codreanu, and M. Juntti, "Distributed joint resource and routing optimization in wireless sensor networks via alternating direction method of multipliers," *IEEE Trans. Wireless Commun.*, vol. 12, no. 11, pp. 5454–5467, Nov. 2013.

[27] C. Song, S. Yoon, and V. Pavlovic, "Fast ADMM algorithm for distributed optimization with adaptive penalty," in *Proc. AAAI*, Phoenix, AZ, USA, 2016, pp. 753–759.

[28] S. Boyd, N. Parikh, E. Chu, B. Peleato, and J. Eckstein, "Distributed optimization and statistical learning via the alternating direction method of multipliers," *Found. Trends® Mach. Learn.*, vol. 3, no. 1, pp. 1–122, 2011.

[29] "CC2500 low-cost low-power 2.4 GHz RF transceiver," Data Sheet, Texas Instrum., Dallas, TX, USA, 2011.

[30] A. Sridharan and B. Krishnamachari, "Maximizing network utilization with max-min fairness in wireless sensor networks," *Wireless Netw.*, vol. 15, no. 5, pp. 585–600, 2009.

[31] W.-H. Wang, M. Palaniswami, and S. H. Low, "Application-oriented flow control: Fundamentals, algorithms and fairness," *IEEE/ACM Trans. Netw.*, vol. 14, no. 6, pp. 1282–1291, Dec. 2006.

[32] *Measurement and Instrumentation Data Center (MIDC)*, Nat. Renew. Energy Lab., U.S. Dept. Energy, Washington, DC, USA. Accessed: Dec. 1, 2017. [Online]. Available: https://midcdmz.nrel.gov

[33] W. Xu, W. Cheng, Y. Zhang, Q. Shi, and X. Wang, "On the optimization model for multi-hop information transmission and energy transfer in TDMA-based wireless sensor networks," *IEEE Commun. Lett.*, vol. 21, no. 5, pp. 1095–1098, May 2017.


**Lei Tao** received the B.S. and Ph.D. degrees in computer science and technology from the University of Science and Technology of China, Hefei, China, in 2014 and 2019, respectively. His research interest is wireless networks.

**Xin Ming Zhang** (M'08–SM'18) received the B.E. and M.E. degrees in electrical engineering from the China University of Mining and Technology, Xuzhou, China, in 1985 and 1988, respectively, and the Ph.D. degree in computer science and technology from the University of Science and Technology of China, Hefei, China, in 2001. Since 2002, he has been with the faculty of the University of Science and Technology of China, where he is currently a Professor with the School of Computer Science and Technology. He is also with the National Mobile Communications Research Laboratory, Southeast University, Nanjing, China. From 2005 to 2006, he was a Visiting Professor with the Department of Electrical Engineering and Computer Science, Korea Advanced Institute of Science and Technology, Daejeon, South Korea. He has published over 100 papers in wireless ad hoc and sensor networks. His research interest includes wireless networks. He was a recipient of the Second Prize of Science and Technology Award of Anhui Province of China in Natural Sciences in 2017.

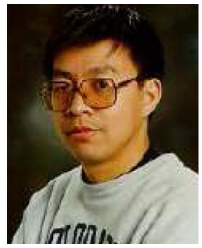

**Weifa Liang** (M'99–SM'01) received the B.Sc. degree in computer science from Wuhan University, China, in 1984, the M.E. degree in computer science from the University of Science and Technology of China in 1989, and the Ph.D. degree in computer science from Australian National University in 1998, where he is currently a Full Professor. His research interests include design and analysis of energy-efficient routing protocols for wireless ad hoc and sensor networks, mobile edge computing and cloud computing, software-defined networking, online social networks, design and analysis of parallel and distributed algorithms, approximation algorithms, combinatorial optimization, and graph theory.